Complete Regression of Xenograft Tumors upon Targeted Delivery of Paclitaxel *via* Π–Π Stacking Stabilized Polymeric Micelles

Yang Shi,[†] Roy van der Meel,[‡] Benjamin Theek,[§] Erik Oude Blenke,[†] Ebel H. E. Pieters,[†] Marcel H. A. M. Fens,[‡] Josef Ehling,[§] Raymond M. Schiffelers,[‡] Gert Storm,[†,∥] Cornelus F. van Nostrum,[†] Twan Lammers,[†,§,∥] and Wim E. Hennink*[,†]

[†]Department of Pharmaceutics, Utrecht Institute for Pharmaceutical Sciences (UIPS), Utrecht University, Utrecht 3584 CG, The Netherlands, [‡]Department of Clinical Chemistry and Haematology, University Medical Center Utrecht, Utrecht 3584 CX, The Netherlands, [§]Department of Experimental Molecular Imaging (ExMI), Helmholtz Institute for Biomedical Engineering, RWTH Aachen University Clinic, Aachen 52074, Germany, and [∥]Department of Targeted Therapeutics, MIRA Institute for Biomedical Technology and Technical Medicine, University of Twente, Enschede 7500 AE, The Netherlands

ABSTRACT Treatment of cancer patients with taxane-based chemotherapeutics, such as paclitaxel (PTX), is complicated by their narrow therapeutic index. Polymeric micelles are attractive nanocarriers for tumor-targeted delivery of PTX, as they can be tailored to encapsulate large amounts of hydrophobic drugs and achiv prolonged circulation kinetics. As a result, PTX deposition in tumors is increased, while drug exposure to healthy tissues is reduced. However, many PTX-loaded micelle formulations suffer from low stability and fast drug release in the circulation, limiting their suitability for systemic drug targeting. To overcome these limitations, we have developed PTX-loaded micelles which are stable without chemical cross-linking and covalent drug attachment. These micelles are characterized by excellent loading capacity and strong drug retention, attributed to $\pi-\pi$ stacking interaction between PTX and the aromatic groups of the polymer chains in the micellar core. The micelles are based on methoxy poly(ethylene glycol)-*b*-(*N*-(2-benzoyloxypropyl)methacrylamide) (mPEG-*b*-p(HPMAm-Bz)) block copolymers, which improved the pharmacokinetics and the biodistribution of PTX, and substantially increased PTX tumor accumulation (by more than 2000%; as compared to Taxol or control micellar formulations). Improved biodistribution and tumor accumulation were confirmed by hybrid μCT-FMT imaging using near-infrared labeled micelles and payload. The PTX-loaded micelles were well tolerated at different doses, while they induced complete tumor regression in two different xenograft models (*i.e.*, A431 and MDA-MB-468). Our findings consequently indicate that $\pi-\pi$ stacking-stabilized polymeric micelles are promising carriers to improve the delivery of highly hydrophobic drugs to tumors and to increase their therapeutic index.

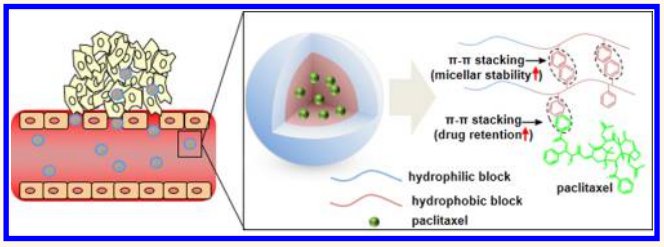

KEYWORDS: nanomedicine · drug targeting · polymeric micelles · paclitaxel · $\pi-\pi$ stacking

Taxane-based chemotherapeutic agents, such as paclitaxel (PTX) and docetaxel, are clinically well-established mitotic inhibitors that present high therapeutic efficacy against a range of solid tumors. The application of taxane-based therapies in patients is hampered by dose-limiting neurotoxic adverse effects, as well as by the highly hydrophobic nature of the molecules, which requires them to be administered in solubilization enhancers, such as Cremophor EL, which are typically associated with hypersensitivity reactions.[1]

To improve the solubility and therapeutic efficacy, and reduce adverse effects of taxanes, drug carriers based on polymer conjugates and nanoparticles have been employed.[2−9] Polymeric micelles are ideal carrier systems for the development of anticancer nanomedicines as they can be synthesized from polymers suitable for systemic administration in humans, customized to encapsulate drugs at doses used in clinical practice and tailored to achiv prolonged circulation kinetics necessary for tumor accumulation.[10−16] Several polymeric micelle-based nanomedicines are being evaluated in (pre)clinical studies for cancer therapy,[17−19] and PTX-loaded monomethoxy poly(ethylene glycol)-*block*-poly(D,L-lactide)

* Address correspondence to W.E.Hennink@uu.nl.

Received for review November 6, 2014 and accepted April 1, 2015.

Published online April 01, 2015
10.1021/acsnano.5b00929

(mPEG−PDLLA) based polymeric micelles (Genexol PM/Cynviloq/IG-001) have been approved for the treatment of various cancers in several countries in Asia.[20,21] Because of the favorable biocompatibility of mPEG−PDLLA, the Genexol-PM formulation showed a significantly decreased toxicity as compared to Cremophor-based Taxol.[20,22]

Although current PTX-polymeric micelle formulations significantly improve PTX solubility and decrease its toxicity, their therapeutic efficacy is comparable to Taxol. Indeed, it has been frequently observed that PTX encapsulated in polymeric micelles has similar pharmacokinetics as does the free drug,[23,24] which is caused by destabilization of the micelles after intravenous (iv) injection,[25,26] as well as by rapid PTX release from the micelles.[23,24] Because of the poor stability and drug retention of current PTX-loaded polymeric micelles, the potential of these nanocarrier systems to increase therapeutic efficacy by making use of the enhanced permeability and retention (EPR) effect is not properly exploited.[14,27−31]

The dissociation of polymeric micelles can be prevented by chemical cross-linking,[32] but this strategy does not necessarily improve drug retention within the micelles. Chemical conjugation of drug molecules to polymeric micelles has been shown to be an effective method to increase the drug retention in polymeric micelles, but such approaches tend to be technically challenging and can adversely affect the pharmacological effect of the drugs.[33−36]

We previously demonstrated that incorporation of aromatic methacrylamide monomers in the hydrophobic block of thermosensitive polymers based on methoxy poly(ethylene glycol)-*b*-(*N*-(2-lactoyloxypropyl)methacrylamide) (mPEG-*b*-p(HPMAm-Lac) can considerably improve the stability, drug loading capacity and drug retention of taxane-loaded polymeric micelles, which was attributed to $\pi-\pi$ stacking interactions between the drug and the aromatic groups of the polymer chains.[37] However, these aromatic thermosensitive polymeric micelles showed insufficient stability in the blood circulation after iv injection, reflected by the quick decrease of the plasma concentration of PTX loaded in the micelles.

In the current study, we show that by increasing the amount of aromatic substitution of the HPMAm repeating units in the block copolymer of mPEG-*b*-pHPMAm, the polymer (methoxy poly(ethylene glycol)-*b*-(*N*-(2-benzoyloxypropyl) methacrylamide)) (mPEG-*b*-p(HPMAm-Bz)) forms micelles with greatly enhanced micellar stability and PTX retention in the blood circulation. These favorable properties are attributed to noncovalent $\pi-\pi$ stacking interactions, while previously it was necessary to apply chemical cross-linking and covalent drug conjugation for stabilizing micelles and increasing drug retention.[35,38] The physicochemical properties of the obtained PTX-loaded micelles were characterized, after which circulation kinetics and biodistribution in tumor-bearing mice were determined by multimodal imaging techniques and ultra performance liquid chromatography (UPLC) analysis. The newly developed $\pi-\pi$ stacked PTX-loaded polymeric micelles displayed prolonged circulation kinetics and improved tumor accumulation as compared to Taxol and control micelles, and they induced complete tumor regression in two different xenograft models, at low doses of PTX and without causing significant side effects.

RESULTS AND DISCUSSION

Synthesis and Characterizations of mPEG-*b*-p(HPMAm-Bz). The polymer used to prepare $\pi-\pi$ stacked polymeric micelles, *i.e.*, mPEG-*b*-p(HPMAm-Bz), was synthesized by free radical polymerization *via* a macroinitiator route (Figure 1A).[37,39] The polymer was obtained in a high yield after purification (70%). GPC analysis showed that the M_n of the synthesized polymers was 20 kDa (which is close to that calculated based on ^{1}H NMR analysis (Supporting Information Figure S1A); 22 kDa), and the polydispersity index (PDI, M_w/M_n) was 1.7. Previous studies have shown that amphiphilic polymers with relatively high molecular weight distribution (PDI $\approx$ 1.7) form micelles with similar characteristics regarding size, size distribution and loading capacity as compared to micelles prepared based on polymers synthesized by controlled/living polymerizations techniques.[37,40,41] Furthermore, from a pharmaceutical and translational point of view, polymers synthesized by free radical polymerization have advantages such as ease and cost-effectiveness of synthesis, high scale-up feasibility, and no necessity for using toxic reagents, such as copper catalysts.

The critical micelle concentration (CMC) of the polymer was 1.3 μg/mL, as measured using pyrene as a fluorescent probe.[39] The CMC of mPEG-*b*-p(HPMAm-Bz) was substantially lower as compared to that of methoxy poly(ethylene glycol)-*b*-(*N*-(2-benzoyloxy$_{30}$)-methacrylamide)-*co*-(*N*-(2-lactoyloxypropyl)methacrylamide$_{70}$) (mPEG-*b*-p(HPMAm-Bz$_{30}$-*co*-HPMAm-Lac$_{70}$)) (CMC was 20 μg/mL[37]). This very low CMC is likely attributed to strong $\pi-\pi$ stacking and hydrophobic interactions between the polymer chains.

To label mPEG-*b*-p(HPMAm-Bz) with the near-infrared (NIR) fluorophore Cy7 for *in vivo* optical imaging studies, mPEG-*b*-p(HPMAm-Bz) with 2 mol % (relative to HPMA-Bz) of *N*-(2-aminoethyl)methacrylamide hydrochloride (AEMAm) was synthesized and reacted with Cy7 NHS ester *via* the amine-NHS reaction (Figure 1B and C). After 48 h of reaction, 84% of the primary amine groups of the polymer had reacted with Cy7 NHS ester. After the coupling reactions, on average, one polymer chain carried one Cy7 label. ^{1}H NMR spectrum (Supporting Information Figure S1B) and GPC chromatograms (Supporting Information Figure S2)

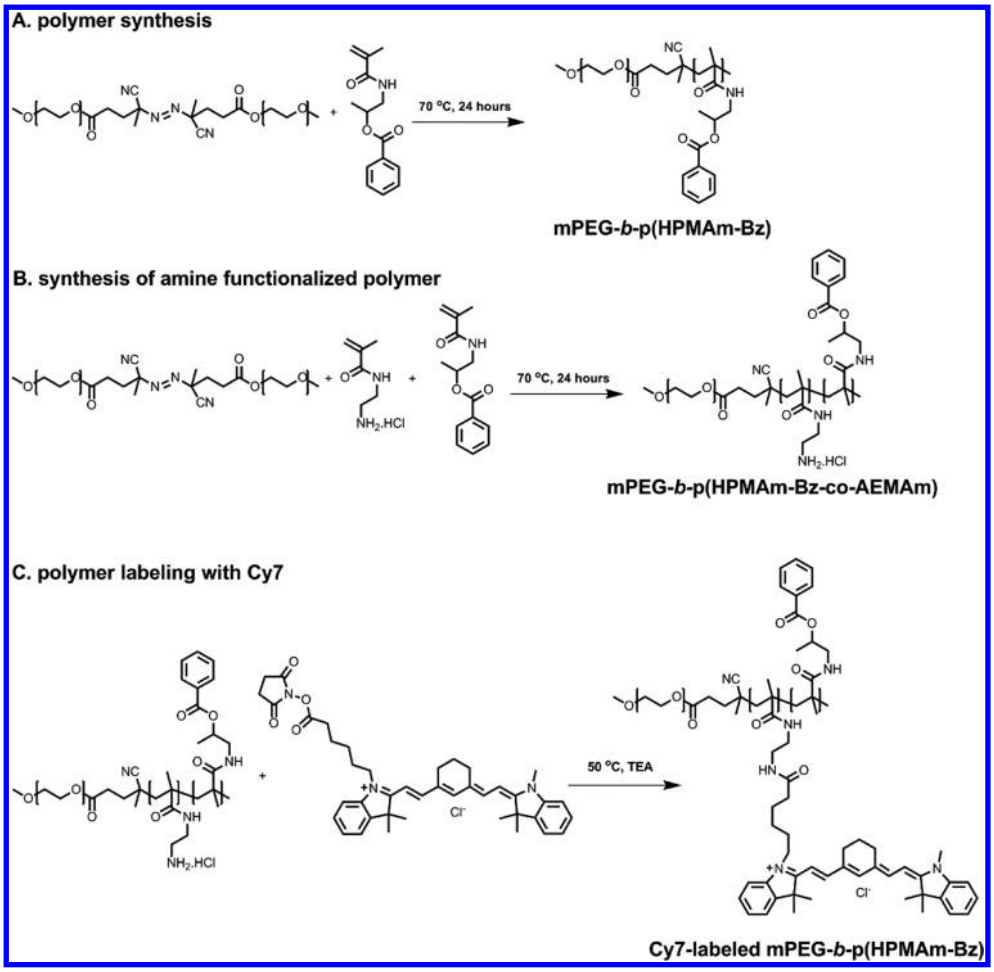

Figure 1. Synthesis and Cy7 labeling of mPEG-*b*-p(HPMAm-Bz). (A) Polymer synthesis; (B and C) Cy7 labeling.

of the Cy7-labeled polymer are shown in the Supporting Information.

Preparation of $\pi-\pi$ Stacked mPEG-*b*-p(HPMAm-Bz) Micelles Loaded with PTX. Polymeric micelles of mPEG-*b*-p(HPMAm-Bz) were prepared by dropwise adding a THF solution of polymer and PTX into water followed by evaporation of THF. The amount of THF left after evaporation for 48 h was 3 wt % as measured by NMR analysis. The residual amount of THF (which did not result in any *in vitro* and *in vivo* toxicity) can be removed by lyophilization, as routinely performed for formulations used in the clinic, such as NK105 and Genexol-PM. Immediately after mixing the polymer solution with water, the *Z*-average particle size (Z_{ave}) of the particles as measured by DLS was 120 nm (PDI of 0.11), which decreased to 71 nm (PDI of 0.08) after evaporation of THF for 48 h. Therefore, the micelles were already formed after mixing the polymer solution with water (50 vol % of THF in the micellar dispersion) and the particles became smaller because THF gradually evaporated. The polymeric micelles showed a high encapsulation efficiency (>80%) at a PTX feed concentration <10 mg/mL, and the highest loading capacity was 23 wt %, at a feed PTX concentration of 10 mg/mL (Figure 2A), which is much higher than that achieved with other micellar nanomedicine formulations (*e.g.*, Genexol-PM[42]). We did not attempt to further enhance the loading capacity of our formulation (as, *e.g.*, in Schulz *et al.*[2]), but primarily aimed to develop a micellar nanocarrier that is stable in systemic circulation, and that efficiently retains PTX within the micellar core during transit from the site of injection to the tumor. The PTX-loaded polymeric micelles, dependent on the PTX content, had a greater size than that of empty micelles, ranging from 79 to 104 nm with low PDI (<0.15) (Figure 2B). The micelles were able to retain PTX, releasing 30% of the loaded drug in 10 days in PBS at 37 °C (Supporting Information Figure S3).

Effects of Empty and PTX-Loaded Polymeric Micelles on Cell Viability. Cell viability assays were performed with A431 and MDA-MB-468 tumor cells to assess the cytocompatibility of the developed micellar formulation and to determine the therapeutic efficacy of PTX-loaded micelles as compared to Taxol *in vitro*. Figure 3A shows that the viability of A431 and MDA-MB-468 tumor cells was completely suppressed at Cremophor EL (Taxol vehicle) concentrations of 0.01 and 0.001 mg/mL, respectively, while both types of cells were fully viable at the micelle concentrations up to 0.5 mg/mL.

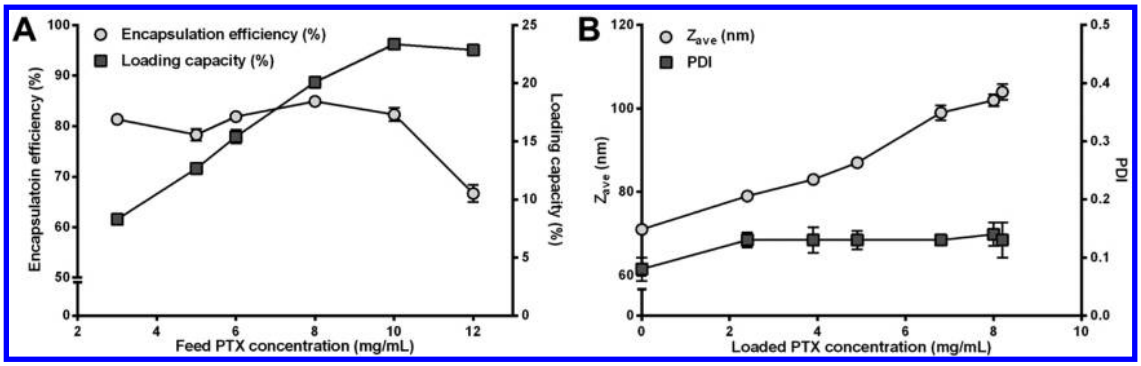

Figure 2. Characterization of the mPEG-*b*-p(HPMAm-Bz) micelles loaded with PTX. (A) Encapsulation efficiency and loading capacity; (B) Z_{ave} and PDI. Data are presented as mean ± SD.

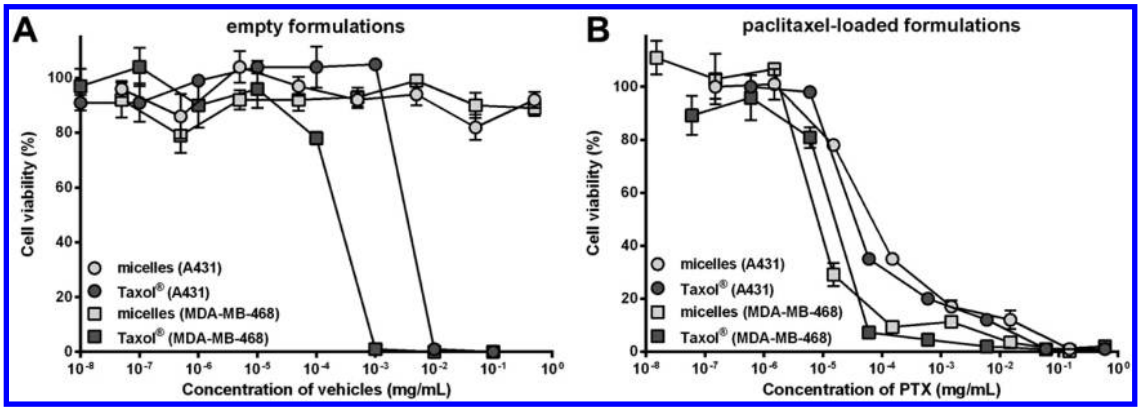

Figure 3. Viability of A431 and MDA-MB-468 tumor cells after exposure to polymeric micelles and Taxol for 72 h. (A) Exposure to empty formulations; (B) exposure to PTX-loaded formulations. Data are presented as mean ± SD.

These results suggest a favorable toxicity profile of the empty polymeric micelles when compared to Cremophor EL.

Figure 3B shows that the effects of PTX-loaded polymeric micelles on tumor cell viability were comparable to those of Taxol (IC_{50} of PTX in polymeric micelles and Taxol were 76 and 42 nM in A431 cells, and 10 and 18 nM in MDA-MB-468 cells, respectively). These results show that the micellar encapsulation of PTX did not decrease the potency of the drug *in vitro*. The micellar PTX is able to induce cytotoxic effects after being released from the carriers either extracellularly or intracellularly during the incubation with the cells, which results in similar therapeutic efficacy as compared to Taxol.[43]

Biodistribution of $\pi-\pi$ Stacked Cy7-Labeled mPEG-*b*-p-(HPMAm-Bz) Micelles Loaded with Cy5.5 by Multimodal Imaging Techniques. The circulation kinetics and biodistribution of the Cy7-labeled mPEG-*b*-p(HPMAm-Bz) micelles loaded with Cy5.5 (preparation and characterization are described in Section 2, Supporting Information) after iv injection into mice bearing A431 tumors were assessed using 2D fluorescence reflectance imaging (FRI) and a newly developed hybrid imaging technique, *i.e.*, noninvasive 3D microcomputed tomography-fluorescence molecular tomography (μCT-FMT), which allows for a more accurate quantification of the biodistribution of fluorophores in mice.[44,45] Figure 4A shows the prolonged blood circulation of mPEG-*b*-p(HPMAm-Bz) micelles labeled with Cy7. Cy5.5 as a model drug had faster elimination kinetics than those of the micelles, which suggests some initial burst release of the Cy5.5 from the micelles in the blood circulation. Nevertheless, the *in vivo* behavior of the model drug and the micelles were closely associated, as evidenced by their relatively similar biodistribution assessed by μCT-FMT (Figure 4B) and colocalization of Cy7 and C5.5 in the tumor (Figure 4C).

The biodistribution of Cy7 and Cy5.5 is shown in Figure 4D,E. Substantial tumor accumulation of the micelles (~12 ID%/cm^3 at 48 h post injection) was measured, although the accumulation of the Cy7-labeled polymeric micelles was observed in liver, in line with previous studies.[38,46,47] At the same time, Cy7 could also be detected in kidneys, due to the liberation of some Cy7-labeled polymer chains from the micelles, which subsequently accumulated in the kidneys.[48,49] Whereas iv administered free Cy5.5 is known to be immediately excreted and unable to accumulate in tumors,[50] the tumor accumulation of Cy5.5 entrapped within the $\pi-\pi$ stacked polymeric micelles was almost 8% ID/cm^3 tumor. This result indicates that, in spite of some initial burst release of Cy5.5, the biodistribution and tumor accumulation of compounds entrapped in

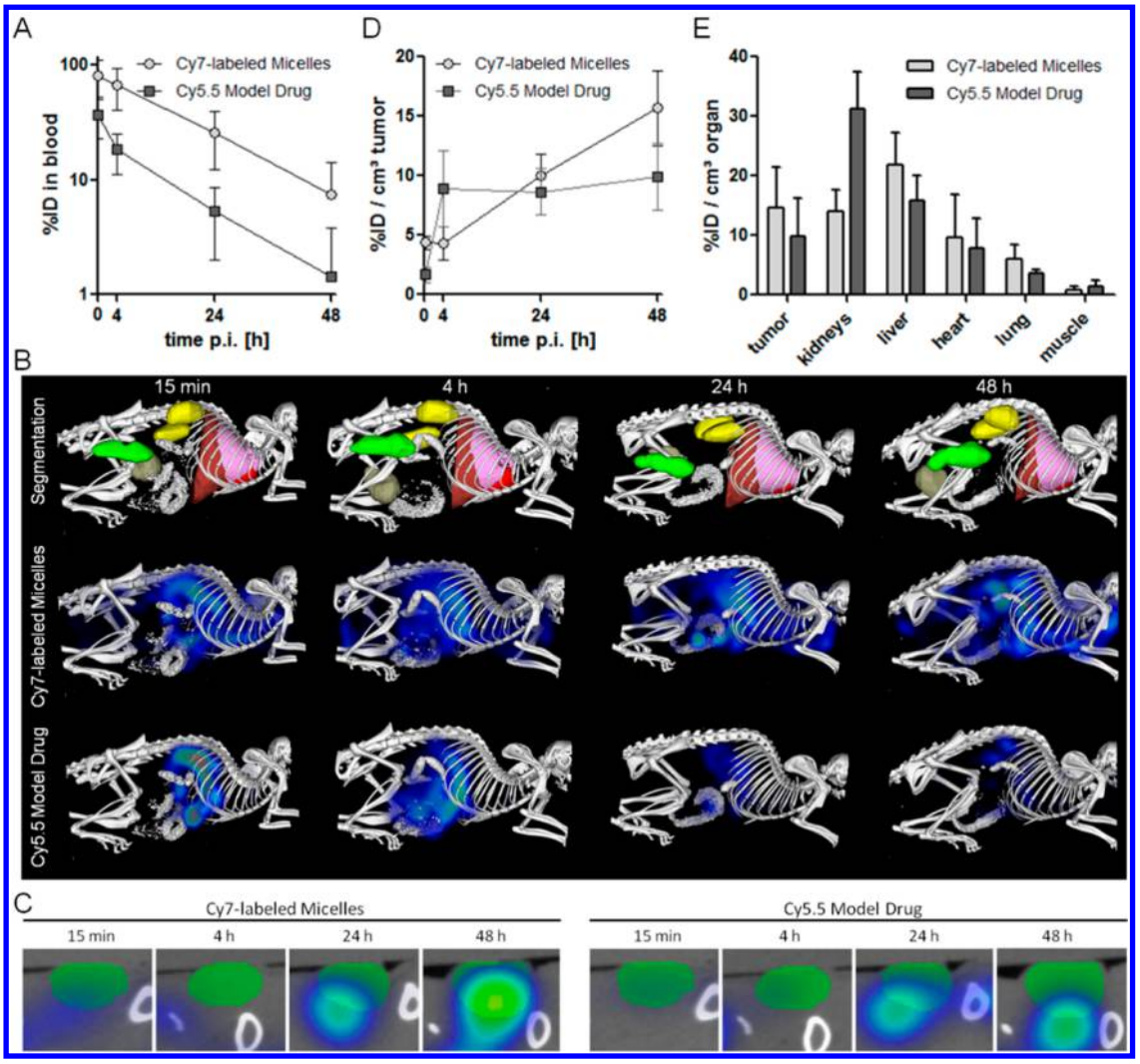

Figure 4. Circulation kinetics and biodistribution of Cy7-labeled mPEG-*b*-p(HPMAm-Bz) micelles loaded with Cy5.5 as a model drug. (A) Blood samples taken at different time points were used to quantify the %ID present in systemic circulation. (B) Representative biodistribution images over time, showing CT-segmented organs and the respective FMT reconstructions of the Cy7-labeled micelle and the Cy5.5 model drug payload. (C) Transversal slice through the tumor, exemplifying the efficient accumulation of both the Cy7-labeled micelles and the Cy5.5-based model drug at the pathological site. (D) Quantification of the %ID accumulating in tumors over time. (E) Accumulation of the Cy7-labeled micelles and the Cy5.5-based model drug in tumors and healthy tissues at 48 h post iv injection. Data are presented as mean ± SD (n = 5).

the micelles are still markedly improved, confirming the ability of long circulating polymeric micelles to facilitate drug targeting to tumors *via* the EPR effect.[51−53]

Ex vivo FRI shows prominent accumulation of the Cy7-labeled polymeric micelles in the tumor, as well as in the liver, kidney and spleen (Figure 5A and B), which is in line with the biodistribution of Cy7-labeled polymeric micelles by *in vivo* μCT-FMT imaging (Figure 4E). The high accumulation of the polymeric micelles in the spleen is consistent with previous studies.[38] Similar to the *in vivo* μCT-FMT imaging data, the accumulation of Cy5.5 in these organs was lower than that of Cy7, which can be ascribed to some burst release and therefore elimination of Cy5.5 from the blood circulation. Figure 5B shows that, apart from the deposition of Cy5.5 in kidneys,[50] the highest level of the model drug was delivered to tumor, which means that the relative tumor deposition of the model compound was greatly improved by the polymeric micelles.

Pharmacokinetics and Biodistribution of PTX-Loaded $\pi-\pi$ Stacked mPEG-*b*-p(HPMAm-Bz) Micelles in a Human Tumor Xenograft Model. Following iv injection, quick elimination of PTX loaded in polymeric micelles or other nanosized particulate formulations, *e.g.*, PEGylated liposomes, in the blood circulation hampers tumor-targeted drug delivery exploiting the EPR effect.[54−56] One explanation for these observations is that polymeric micelles quickly dissociate in systemic circulation due to disturbance of the unimer-micelle equilibrium by plasma proteins which bind unimers.[38] However, even by using stable polymeric micelles (MePEG$_{114}$-*b*-PCL$_{104}$ or core-cross-linked mPEG-*b*-p((20%HEMAm-Lac$_1$)-*co*-(80%HEMAm-Lac$_2$)) with long circulation times in the bloodstream, it was found that physically

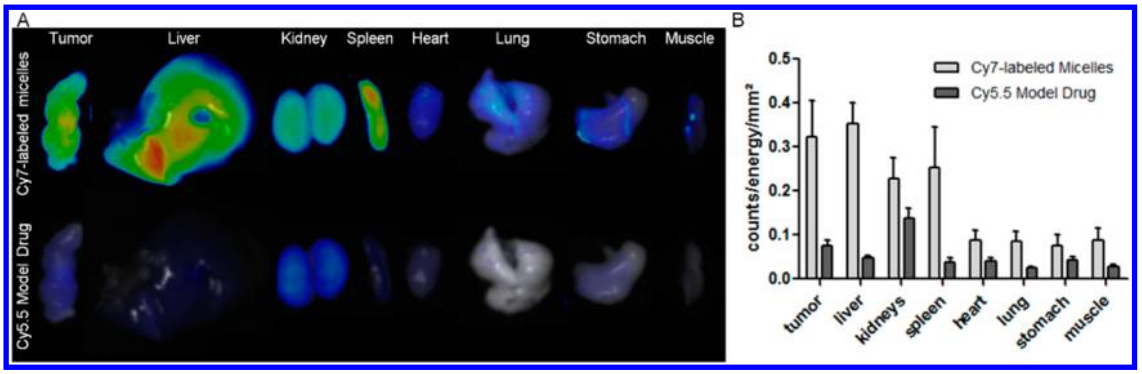

Figure 5. *Ex vivo* **FRI analysis of the accumulation of the Cy7-labeled micelles and the Cy5.5-based model drug in tumors and healthy organs. (A) Representative images, obtained at wavelengths of 750 nm (micelles) and 680 nm (model drug) are shown. (B) Quantification of the** *ex vivo* **images of micelle and model drug accumulation exemplify effective and relatively selective targeting to tumors.**

loaded PTX had an elimination time similar as that of PTX solubilized in Taxol, which is ascribed to a low PTX retention in those micelles.[23,57]

We previously reported that by incorporating aromatic monomers in thermosensitive mPEG-*b*-p(HPMAm-Bz/Nt-*co*-HPMAm-Lac) polymeric micelles, the stability and drug retention were significantly improved as compared to thermosensitive polymeric micelles without aromatic monomers.[37] However, the circulation time of PTX in the aromatic thermosensitive polymeric micelles was still rather short, and similar to that of thermosensitive polymeric micelles without aromatic groups and the Taxol formulation (Supporting Information Figure S5).[56,57]

The pharmacokinetic (PK) profiles of PTX administered in micelles based on mPEG-*b*-p(HPMAm-Bz) polymers and that of Taxol were studied in mice bearing human A431 tumor xenografts. Figure 6A shows that after iv injection, PTX in Taxol was quickly eliminated from the blood circulation and less than 10% of the injected dose was detected in blood 2 min post injection, which is in agreement with previously reported data.[56] Importantly, the half-life of PTX loaded in the mPEG-*b*-p(HPMAm-Bz) micelles was significantly increased (~8 h) when compared to that of Taxol, and considerably higher than that of Cy5.5 model drug which can be explained by the higher loading content of PTX than Cy5.5.[58−60] Overall, these data point to an excellent stability and retention of PTX in micelles based on mPEG-*b*-p(HPMAm-Bz) in the blood circulation. Occurrence of $\pi-\pi$ stacking interactions in micelles has been reported before.[37,61] In a previous study,[37] thermosensitive polymeric micelles based on polymers similar to mPEG-*b*-p(HPMAm-Bz) with a low content (<30 mol %) of aromatic repeating units were analyzed by solid state NMR spectroscopy and the results point to $\pi-\pi$ stacking interactions between aromatic groups in the micellar core. In the present study, polymeric micelles were prepared using mPEG-*b*-p(HPMAm-Bz) with 100 mol % of aromatic repeating units in the hydrophobic block and $\pi-\pi$ stacking interactions between the aromatic groups are expected to occur.

A comparably long half-life of PTX has been reported for micelles based on poly(ethylene glycol)-poly(aspartate) block copolymers modified with 4-phenyl-1-butanol (~6.5 h).[43] The $AUC_{0\text{-inf}}$ of the PTX loaded in the mPEG-*b*-p(HPMAm-Bz) micelles in the blood circulation was ~1800 μg·h/mL, which is in the high range reported in literature for drug-loaded polymeric micelles.[23,62,63] Furthermore, it is markedly higher than that of Taxol formulation (~80 μg·h/mL at a dose of 20 mg/kg)[56] and comparable to that of PTX-loaded long circulating micelles reported previously (~8000 μg·h/mL at around 4 times higher dose of PTX (50 mg/kg).[43]

The biodistribution of PTX 24 h after iv injection of the different formulations in tumor-bearing mice was investigated (Figure 6B). The animals were sacrificed at 24 h after iv injection (without saline perfusion) and PTX levels were determined. Although there was still ~10% of the injected dose of the PTX-loaded micelles present in the systemic circulation at this time point (for mPEG-*b*-p(HPMAm-Bz) micelles), this does not affect the overall biodistribution pattern, as the relative blood volume in tumors is much lower than that in the majority of healthy tissues. PTX could not be detected in the tumors of mice that received PTX formulated in the thermosensitive mPEG-*b*-p(HPMAm-Bz/Nt-*co*-HPMAm-Lac) micelles or Taxol (corresponding to values below 0.4 ID%/g organ). In contrast, high concentration of PTX in tumors (~8 ID%/g at 24 h post injection) of mice that received PTX-loaded mPEG-*b*-p(HPMAm-Bz) micelles was detected. These results confirm the prolonged circulation kinetics for the stable PTX-loaded mPEG-*b*-p(HPMAm-Bz) micelles, whereas PTX formulated as Taxol or encapsulated in the control micelles appears to be rapidly released in the circulation and excreted within 24 h. At doses up to 20 mg/kg, rapid clearance of PTX is frequently observed, resulting in low PTX accumulation in healthy organs at 24 h post iv injection, with values ranging

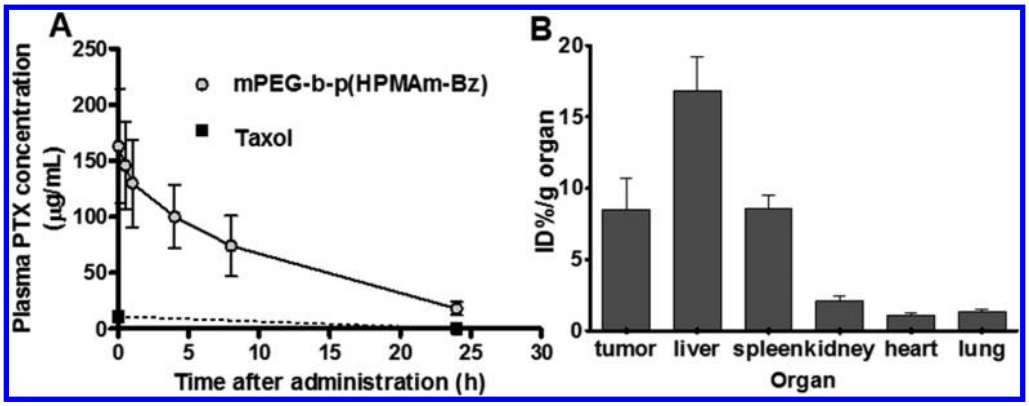

Figure 6. Circulation kinetics and biodistribution of PTX-loaded polymeric micelles (14 mg/kg PTX). (A) Plasma concentrations of PTX after iv injection of different formulations in A431 tumor-bearing mice. PTX concentrations in blood samples from mice that received Taxol or thermosensitive mPEG-*b*-p(HPMAm-Bz/Nt-*co*-HPMAm-Lac) micelles were below the detection limit (<0.6 μg/mL plasma) 24 h post injection. (B) ID%/g organ of PTX in mice 24 h after iv injection of PTX-loaded mPEG-*b*-p(HPMAm-Bz) micelles. PTX concentrations in organs (tumor, liver, kidneys, spleen, heart and lungs) of mice that received Taxol and PTX-loaded thermosensitive mPEG-*b*-p(HPMAm-Bz/Nt-*co*-HPMAm-Lac) micelles were below the detection limit (<0.4 ID%/g organ). Data are presented as mean $\pm$ SD (n = 7−8).

between 0.1 and 2 μg/g tissue.[64,65] These results are in agreement with our findings, in which the tumor and tissue concentrations of PTX administered in free form and control micelles were below the detection limit (*i.e.*, below 2 μg/g). This notion again exemplifies that PTX delivery can be substantially improved upon incorporation in $\pi-\pi$-stacked polymeric micelles. PTX was also found in liver and spleen, in agreement with the imaging data of Cy7 labeled micelles (Figures 4D,E and 5B) and indicating clearance of the micelles by hepatosplenic macrophages.[46] In contrast to Cy5.5 which highly accumulated in kidneys (Figures 4 and 5), PTX did not show substantial deposition in kidneys. PTX accumulation in the tumor (~8% ID%/g) correlated with the results of μCT-FMT study.

Antitumor Efficacy of PTX-Loaded mPEG-*b*-p(HPMAm-Bz) Micelles. The therapeutic efficacy of the PTX-loaded mPEG-*b*-p(HPMAm-Bz) micelles was studied in mice bearing human A431 epidermoid and MDA-MB-468 breast carcinoma xenografts. For the A431 tumor model, treatment was initiated 1 week after inoculation of the tumor cells, when tumors had reached a volume of ~100 mm^3. Mice that received PBS or empty mPEG-*b*-p(HPMAm-Bz) micelles every other day, reached tumor volumes of ~1500 mm^3 in 20 days (Figure 7A). The tumor growth of mice treated with Taxol (15 mg/kg of PTX) was not significantly inhibited compared to that of mice treated with empty micelles or PBS (p > 0.05), which can be ascribed to the low tumor accumulation of PTX. At the same time, an equal dose of PTX (15 mg/kg) loaded in the mPEG-*b*-p-(HPMAm-Bz) micelles fully inhibited tumor growth for at least 33 days. Moreover, in tumor-bearing mice injected with 30 mg/kg of PTX-loaded in mPEG-*b*-p(HPMAm-Bz) micelles, complete tumor regression was observed 35 days after the initial treatment. These results demonstrate that improved tumor-targeted delivery of PTX using polymeric micelles with robust *in vivo* stability and circulation kinetics is crucial to enhance the therapeutic efficacy of PTX.

The survival of mice, defined as reaching the humane end point (tumor volume ≥1500 mm^3), treated with the different PTX formulations is shown in Figure 7B. The survival of mice treated with PTX-loaded mPEG-*b*-p(HPMAm-Bz) micelles (30 or 15 mg/kg) was significantly longer as compared to that of mice treated with the Taxol formulation (p < 0.01).

In the therapeutic efficacy study using MDA-MB-468 breast carcinoma xenografts, mice received similar treatments as in the A431 study but iv injections were administered once a week rather than every other day. Treatment was initiated 4 weeks after inoculation with the tumor cells, when tumors had reached a volume of ~100 mm^3. Figure 7D shows that Taxol (15 mg/kg PTX) only slightly inhibited tumor growth, while the tumors of mice that received the PTX-loaded micelles (15 and 30 mg/kg PTX) decreased in volume and completely regressed after 60 days. These results confirm the potent therapeutic efficacy of the PTX-loaded polymeric micelles observed in the study with A431 as a tumor model.

Repeated injections of PTX-loaded polymeric micelles were generally well tolerated and mice did not suffer from significant weight loss throughout the course of the therapeutic efficacy studies (Figure 7E, F). Furthermore, no organ toxicities were observed for the empty or PTX-loaded polymeric micelles, as representatively assessed for liver, spleen and kidney by histopathological analysis (Supporting Information Figure S6). These observations suggest a favorable toxicity profile for the micellar formulation.

Polymeric micelles with a prolonged circulation time and efficient paclitaxel retention have been described before by Kataoka and colleagues.[43] This formulation, NK105, has been tested in animal models and shown to be safe in patients, and it is currently in

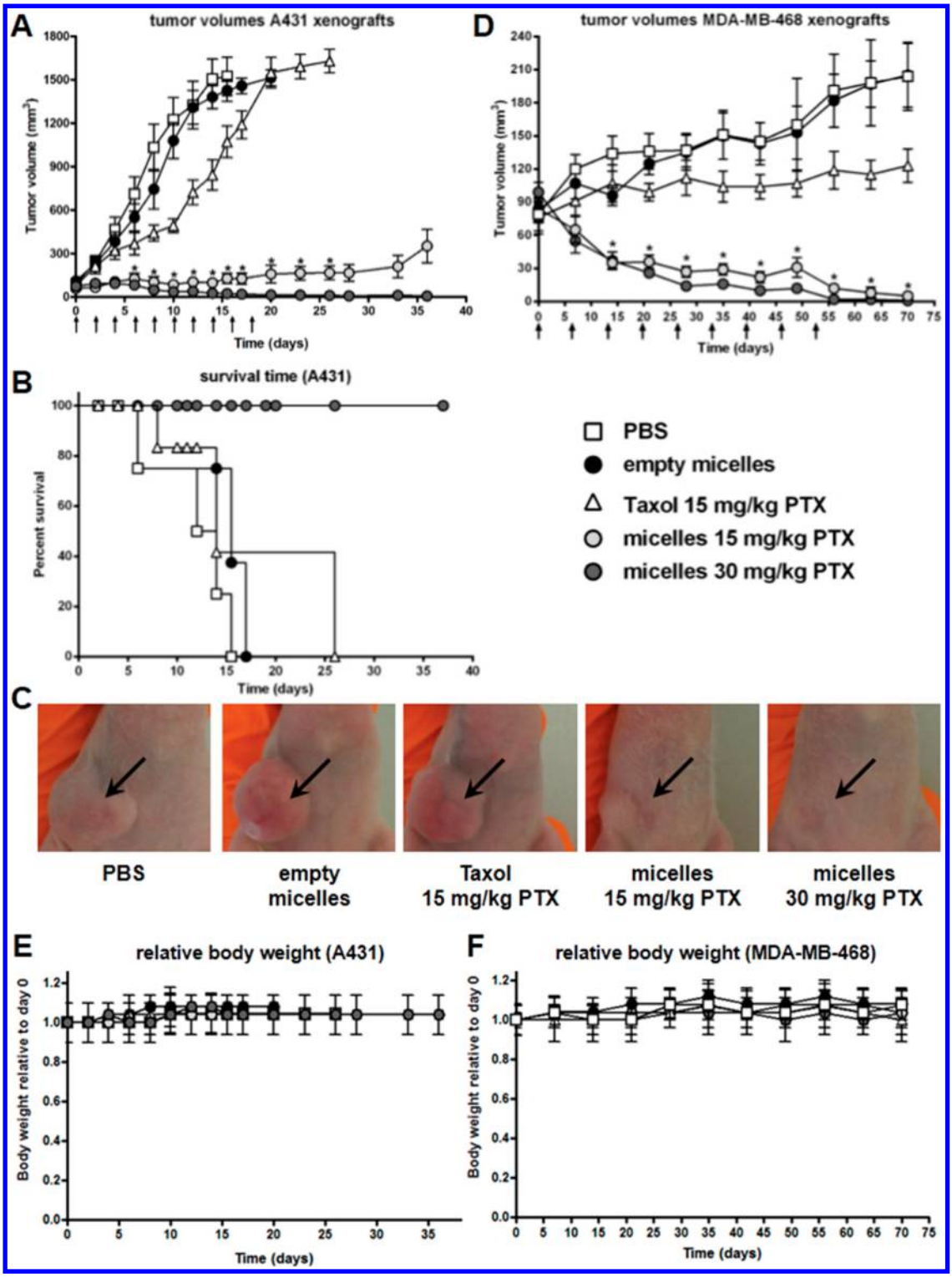

Figure 7. Therapeutic efficacy of PTX-loaded polymeric micelles in human tumor xenograft models. Treatment consisted of iv injections of PBS, empty mPEG-*b*-p(HPMAm-Bz) micelles, Taxol (15 mg/kg PTX) and PTX-loaded mPEG-*b*-p(HPMAm-Bz) micelles (15 and 30 mg/kg PTX). Arrows represent iv injections. (A) Tumor growth of A431 xenografts in mice. Data are presented as mean ± SEM ($n = 12$). Data were statistically analyzed by one-way ANOVA with Bonferroni post-test. *p-value < 0.01 Taxol (15 mg/kg PTX) *versus* micelles (30 or 15 mg/kg PTX), p-value < 0.01 micelles (30 or 15 mg/kg PTX) *versus* PBS or empty micelles. (B) Kaplan−Meier survival curves of A431 tumor-bearing mice treated with PTX formulations or negative control ($n = 12$). Data were statistically analyzed by log rank test. (C) Representative images of A431 tumor-bearing mice 15 days after the first injection. (D) Tumor growth of MDA-MB-468 xenografts in mice. Data are presented as mean ± SEM ($n = 8$). Data were statistically analyzed by one-way ANOVA with Bonferroni post-test. *p-value < 0.01 Taxol (15 mg/kg PTX) *versus* micelles (30 or 15 mg/kg PTX), p-value < 0.01 micelles (30 or 15 mg/kg PTX) *versus* PBS or empty micelles. (E and F) Relative body weight of mice bearing A431 ($n = 12$) and MDA-MB-468 ($n = 8$) xenografts, respectively, throughout therapeutic efficacy studies. Data are presented as mean ± SD.

the final phases of clinical evaluation. When comparing these micelles to our formulation, it should be noted that both systems are based on block copolymers containing pendant aromatic groups. In our case, the polymer was synthesized *via* a simple and straightforward one-step radical polymerization, as opposed to the polymer used in NK105, which was prepared in three steps, involving ring opening polymerization and postpolymerization modifications. Both formulations have similar PTX loading capacity (~23 wt %) and size (80−100 nm). PTX entrapped in our formulation has a slightly longer circulation half-life than that in NK105 (8 *versus* 6.5 h, respectively). Although evaluated in different animal models, the therapeutic potential of both formulations is comparable, inducing complete tumor regression at cumulative PTX doses of ~300 mg/kg. These notions, together with the fact that NK105 has shown promising responses in patients (and will likely be approved for clinical use later on this year), indicate that our formulation holds significant clinical potential, with similar loading capacity and therapeutic efficacy, and with an even longer circulation half-life time. Once NK105 has reached the market, a direct head-to-head comparison to our formulation would be possible, enabling an accurate assessment of the potential of PEG-*b*-p(HPMAm-Bz) micelles.

Taken together, our results demonstrate that the developed polymeric micelles stabilized by $\pi-\pi$ stacking interactions are attractive carrier systems for the development of PTX-nanomedicines. The polymeric micelles are produced in a straightforward and cost-effective manner, without the need for chemical cross-linking or covalent drug conjugation, and are characterized by excellent loading capacity, enhanced stability and strong PTX retention. The IC_{50} values of micellar PTX were comparable to those of the free drug (*i.e.*, Taxol), for both A431 and MDA-MB-468 cells, indicating that the potency of PTX was not compromised by encapsulation. The micellar characteristics ensure prolonged circulation kinetics, substantial tumor accumulation and efficient tumor regression in two well-known and routinely used xenograft models, *i.e.*, A431 and MDA-MB-468, without inducing significant toxicity, demonstrating the therapeutic (and translational) potential of this formulation.

CONCLUSIONS

In this study, an amphiphilic polymer mPEG-*b*-p(HPMAm-Bz) bearing aromatic benzoyl groups was synthesized *via* free radical polymerization. In an aqueous solution, this polymer forms micelles that are characterized by high loading capacity and strong retention of PTX. Cell viability studies indicated that the polymeric micelles had a much better cytocompatibility than Taxol solvent, while PTX loaded in the polymeric micelles displayed comparable cytotoxicity as Taxol. After iv injection, the mPEG-*b*-p(HPMAm-Bz) micelles displayed prolonged blood circulation kinetics and, importantly, efficient PTX retention in the micelles, which is attributed to $\pi-\pi$ stacking and hydrophobic interactions between the polymer chains and PTX. As a result, high tumor accumulation of PTX delivered by the stable polymeric micelles was observed. These results were confirmed by *in vivo* imaging studies with Cy7-labeled polymeric micelles loaded with Cy5.5 as a model drug. The PTX-loaded mPEG-*b*-p(HPMAm-Bz) micelles induced complete regression of both A431 epidermoid and MDA-MB-468 breast carcinoma xenografts, while Taxol only displayed modest therapeutic effects in both models. Repeated injections of empty or PTX-loaded polymeric micelles were generally well tolerated and the mice did not suffer from body weight loss, which points to an acceptable safety profile. Overall, polymeric micelles stabilized by $\pi-\pi$ stacking interactions are consequently considered to be an attractive platform for the development of hydrophobic drug-based nanomedicines.

METHODS AND MATERIALS

The $mPEG_2$-ABCPA macroinitiator (M_n of mPEG = 5000 g/mol) and HPMAm-Bz were synthesized as described previously.[37,66] *N*-(2-Aminoethyl)methacrylamide hydrochloride (AEMAm) was purchased from Polysciences, Inc. Cyanine7 (Cy7) NHS ester and Cyanine5.5 alkyne (Cy5) were ordered from Lumiprobe Corporation. Paclitaxel (PTX) was purchased from LC Laboratories (Woburn, MA, USA). Acetonitrile (ACN), diethyl ether and *N*,*N*-dimethylformamide (DMF) were supplied by Biosolve Ltd. (Valkenswaard, The Netherlands). PEGs for GPC calibration were obtained from Polymer Standards Service-USA Inc. Syringe filters with Nylon membrane (Acrodisc, size of 0.45 μm) were ordered from Pall Corporation. Taxol was purchased from Bristol-Myers Squibb. PBS pH 7.4 (8.2 g of NaCl, 3.1 g of $Na_2HPO_4 \cdot 12H_2O$, 0.3 g of $NaH_2PO_4 \cdot 2H_2O$ per 0.5 L) was ordered from B. Braun Melsungen AG. A431 and MDA-MB-468 cells were purchased from American Type Culture Collection (ATCC, Manassas, VA, USA).

Synthesis and Characterizations of mPEG-*b*-p(HPMAm-Bz). A block copolymer of methoxy poly(ethylene glycol)-*b*-(*N*-(2-benzoyloxypropyl)-methacrylamide)) (mPEG-*b*-p(HPMAm-Bz) was synthesized *via* a macroinitiator route[37,39] using $mPEG_2$-ABCPA as macroinitiator and HPMAm-Bz as monomer (Figure 1A). The monomer was dissolved at a concentration of 0.3 g/mL in ACN (dried on A4 molecular sieves) and the molar ratio of monomer-to-macroinitiator was 200/1. The solution was degassed by flushing with nitrogen for 30 min. The reaction was conducted at 70 °C for 24 h under a nitrogen atmosphere. The polymer was purified by precipitation in diethyl ether and this dissolution/precipitation procedure was repeated twice. The polymer was dried under vacuum at room temperature for 24 h and collected as a white powder. The critical micelle concentration (CMC) of the polymer was measured according to a previously reported method using pyrene as fluorescent probe.[37] Thermosensitive methoxy poly(ethylene glycol)-*b*-(*N*-(2-benzoyloxy$_{30}$/naphthoyloxypropyl$_{25}$) methacrylamide)-*co*-(*N*-(2-lactoyloxypropyl) methacrylamide$_{70/75}$) (mPEG-*b*-p(HPMAm-Bz$_{30}$)/Nt$_{25}$-*co*-HPMAm-Lac$_{70/75}$) composed of 30/25 mol % of HPMAm-benzoate/naphthoate and 70/75 mol % of HPMA-monolactate in the

thermosensitive block was synthesized and characterized as previously reported.[37]

The ^{1}H NMR spectrum of mPEG-*b*-p(HPMAm-Bz) was recorded using a Gemini 300 MHz spectrometer (Varian Associates Inc. NMR Instruments, Palo Alto, CA), using DMSO-d_6 as the solvent. The DMSO peak at 2.5 ppm was used as the reference line. Chemical shifts of mPEG-*b*-p(HPMAm-Bz): 8.0 (b, 2H, aromatic CH), 7.55 (b, 1H, aromatic CH), 7.65 (b, 2H, aromatic CH), 7.35 (b, CO-NH-CH_2), 5.0 (b, NH−CH_2−CH(CH_3)-O-(Bz)), 3.40−3.60 (b, $mPEG_{5000}$ methylene protons, O−CH_2-CH_2), 3.1 (b, NH-CH_2-CH), 0.1−2.0 (b, the rest of the protons are from the methyl and backbone CH_2 protons).

The number-average molecular weight (M_n) of mPEG-*b*-p(HPMAm-Bz) was determined by ^{1}H NMR analysis as follows: (a) the value of the integral of the mPEG protons divided by 448 (the average number of protons per one mPEG chain, M_n = 5000) gives the integral value for one mPEG chain, and (b) the number of HPMAm-Bz units in the polymers was determined from the ratio of the integral of the aromatic protons of HPMAm-Bz (8.0 ppm, 2H, aromatic CH) to the integral of one mPEG chain. The M_n of the hydrophobic block was calculated from the resulting number of HPMAm-Bz units.

GPC was conducted to measure the number-average molecular weight (M_n), weight-average molecular weight (M_w) and polydispersity (PDI, equal to M_w/M_n) of mPEG-*b*-p(HPMAm-Bz), using two serial Plgel 5 μm MIXED-D columns (Polymer Laboratories) and PEGs of narrow molecular weights as calibration standards. The eluent was DMF containing 10 mM LiCl, the elution rate was 0.7 mL/min, and the temperature was 40 °C.[37]

Synthesis and Characterizations of Cy7 Labeled mPEG-*b*-p(HPMAm-Bz). mPEG-*b*-p(HPMAm-Bz-*co*-AEMAm) was synthesized as described above with 2 mol % of AEMAm (*N*-(2-aminoethyl-)methacrylamide hydrochloride, relative to HPMAm-Bz) copolymerized in the hydrophobic block of the polymer (Figure 1B). The primary amine side groups of mPEG-*b*-p-(HPMAm-Bz-*co*-AEMAm) were subsequently reacted with Cy7 NHS ester (Figure 1C). Briefly, Cy7 NHS ester was dissolved in DMSO (dried on 4 Å molecular sieves) at a concentration of 10 mg/mL. The polymer (31 mg) was transferred into a dried flask, and 0.18 mL solution of the Cy7 NHS ester (10 mg/mL) and 1 μL of TEA (dried on 4 Å molecular sieves) were added and the reaction was conducted at 50 °C for 48 h. Uncoupled Cy7 was removed by dialysis against THF/water (1/1, v/v), refreshing the dialysate after 24 h for in total 5 times. The final product was collected after freeze-drying and obtained as a dark green powder after lyophilization and the amount of Cy7 coupled to the polymer was analyzed as previously described by GPC coupled with a UV detector (detection wavelength of 700 nm) with a calibration curve of Cy7 standard solutions according to a previously reported method.[67]

Preparation of Empty and PTX/(Cy5.5)-Loaded (Cy7-Labeled) mPEG-*b*-p(HPMAm-Bz) Micelles, PTX-Loaded Thermosensitive mPEG-*b*-p(HPMAm-Bz_{30}/Nt_{25}-*co*-HPMAm-$Lac_{70/75}$) Micelles. Empty mPEG-*b*-p(HPMAm-Bz) micelles were prepared as follows. mPEG-*b*-p(HPMAm-Bz) was dissolved in THF at a concentration of 27 mg/mL and subsequently, 1 mL of the polymer solution was added dropwise to 1 mL of reverse osmosis (RO) water while stirring. The mixture was incubated at room temperature for 48 h to allow evaporation of THF. The resulting micellar dispersion was filtered through 0.45 μm nylon membrane (Acrodisc). The *Z*-average (Z_{ave}) size of the micelles was measured by dynamic light scattering (DLS) using an ALV/CGS3 system. The amount of residual THF after evaporation for 48 h was measured ^{1}H NMR as follows. THF (4H at 3.60 ppm) was mixed with D_2O (containing 10 mg/mL sodium acetate as an internal standard), and the amount of THF left after evaporation for 48 h at room temperature was calculated by comparing the integral of THF at 3.60 ppm to that of sodium acetate (CH_3 at 1.76 ppm).

PTX-loaded micelles were prepared similarly as the empty micelles, with PTX dissolved (concentration ranging from 3 to 12 mg/mL) in the polymer solution in THF. The PTX-loaded micelles were filtered through 0.45 μm nylon membrane (Acrodisc) to remove nonencapsulated PTX. To assess the PTX loading content, the PTX-loaded polymeric micelles were diluted with ACN at least 10 times to destabilize the micelles and the dissolved PTX was subsequently quantified by UPLC analysis using Waters Acquity system. Eluent A: ACN/water = 45/55 (v/v) with 0.1% formic acid. Eluent B: ACN/water = 90/10 (v/v) with 0.1% formic acid. A gradient was run with the volume fraction of eluent B increasing from 0 to 100% from 4.5 to 7 min and subsequently decreasing to 0% from 7.5 to 10 min. An ACQUITY UPLC HSS T3 column was used and the detection wavelength was 227 nm. Seven microliters of the solution was injected and the PTX concentration in the different samples was calculated using a calibration curve of PTX standards prepared in ACN in a concentration range of 0.2−100 μg/mL.

The PTX-loaded thermosensitive mPEG-*b*-p(HPMAm-Bz_{30}/Nt_{25}-*co*-HPMAm-$Lac_{70/75}$) micelles were prepared using a fast heating method as previously described[37] with 4.2 mg/mL of feed PTX concentration and 9 mg/mL of polymer concentration, and characterized by Z_{ave} (DLS) and PTX content (UPLC analysis).

For multimodal *in vivo* and *ex vivo* imaging studies, mPEG-*b*-p(HPMAm-Bz) micelles chemically labeled with Cy7 and physically loaded with Cy5.5 were prepared similarly to the PTX-loaded mPEG-*b*-p(HPMAm-Bz) micelles. Briefly, 1 mL THF solution of 26.6 mg of nonlabeled mPEG-*b*-p(HPMAm-Bz), 0.4 mg of Cy7 labeled mPEG-*b*-p(HPMAm-Bz) and 0.02 mg of Cy5.5 (as a physically loaded modal drug) was added dropwise to 1 mL of water while stirring. The micellar dispersion was incubated at room temperature for 48 h to allow evaporation of THF. Next, the resulting micellar dispersion was filtered through 0.45 μm nylon membrane (Acrodisc).

Effects of Empty and PTX-Loaded Polymeric Micelles and Taxol on Cell Viability. The cytocompatibiltiy of empty polymeric micelles and the therapeutic efficacy of PTX-loaded polymeric micelles were evaluated using A431 and MDA-MB-468 cells. Empty and PTX-containing Taxol were used as the control formulations. A431 cells were cultured in Dulbecco's Modified Eagle's Medium (abbreviated as DMEM, PAA Laboratories GmbH, Pasching, Austria) containing 3.7 g/L sodium bicarbonate, 4.5 g/L L-glucose, 2 mM L-glutamine, and supplemented with 10% (v/v) fetal bovine serum (FBS). MDA-MB-468 cells were cultured in ATCC-formulated Leibovitz's L-15 Medium (ATCC, Manassas, VA, USA) supplemented with 10% (v/v) FBS. Cells were kept in culture at 37 °C in a humidified atmosphere containing 5% CO_2. Cells were seeded into 96-well plates at a density of (5×10^3 cells/well) and incubated for 24 h at 37 °C in a 5% CO_2 humidified atmosphere. Stock solutions of empty micelles (polymer = 27 mg/mL) and PTX loaded micelles (varied PTX concentration, polymer = 27 mg/mL) were prepared as described above. Empty Taxol vehicle was prepared by mixing Cremophor EL and ethanol (1/1, v/v). The empty and PTX-loaded micellar and Taxol formulations were diluted in the corresponding cell culture media to yield different concentrations of vehicles and PTX. A volume of 100 μL of the different formulations was added to the wells. The cells were incubated at 37 °C in a humidified atmosphere with 5% CO_2 and the cell viability was determined using a XTT colorimetric assay after 72 h.[37]

Circulation Kinetics and Biodistribution of Cy7-Labeled mPEG-*b*-p-(HPMAm-Bz) Micelles Loaded with Cy5.5 by Multimodal *in Vivo* and *ex Vivo* Imaging. CD-1 nude female mice (n=5) were fed with chlorophyll-free food pellets and water ad libitum, and caged in ventilated cages and clinically controlled rooms and atmosphere. The animal studies were performed in compliance with guidelines set by national regulations and were approved by the local animal experiments ethical committee. CD-1 nude mice were inoculated with A431 tumor cells (4×10^6 cells/100 μL PBS pH 7.4) subcutaneously into the right flank 15 days before the start of the experiment, which led to the development of A431 tumor xenograft with an approximate size of 6−7 mm in width.

In vivo imaging: Cy7-labeled mPEG-*b*-p(HPMAm-Bz) micelles loaded with Cy5.5 were studied for their blood circulation kinetics and biodistribution. The mPEG-*b*-p(HPMAm-Bz) micelles (2.0 nmol Cy7 and 2.5 nmol of Cy5.5) were iv injected into mice under anesthesia using isoflurane. μCT (Tomoscope DUO; CT Imaging, Erlangen, Germany) and 3D FMT imaging (FMT2500; PerkinElmer) were performed immediately after

injection according to the previously reported protocol.[44] The obtained μCT and FMT scans were fused (workflow shown in Supporting Information Figure S4). On the basis of the μCT data, tumor, kidneys, liver, heart, lungs and muscle were segmented, using an Imalytics Research Workstation software (Philips Technologie GmbH Innovative Technologies, Aachen, Germany). Accumulation in spleen, known to be an important organ for clearing nanocarriers from the blood, could not be assessed using μCT-FMT. FMT reconstructed signals were overlapped onto respective organ-segmented μCT images, and the amount of Cy7 and Cy5.5 accumulated in these organs was quantified.

For the circulation kinetics study, blood samples were collected at 2 min, and at 4, 24, and 48 h post injections, and the amount of Cy7 and Cy5.5 in the blood samples was quantified by 2D Fluorescence reflectance imaging (FRI) using a calibration curve.

Ex vivo imaging: The mice that received iv injections of Cy7-labeled mPEG-*b*-p(HPMAm-Bz) micelles loaded with Cy5.5 were sacrificed 48 h after injections. Organs were collected, weighted and analyzed by 2D FRI at the 680 and 750 nm channels.

Pharmacokinetics and Biodistribution of PTX Loaded in mPEG-*b*-p(HPMAm-Bz), Thermosensitive mPEG-*b*-p(HPMAm-Bz$_{30}$/Nt$_{25}$-*co*-HPMAm-Lac$_{70/75}$) Micelles, and Taxol in a Human Tumor Xenograft Model. Female Crl:NU-*Fox^{nu}*1nu mice (22.5 $\pm$ 2.5 g) were purchased from Charles River International Laboratories, Inc. and had free access to water and food. The animal studies were performed in compliance with guidelines set by national regulations and were approved by the local animal experiments ethical committee. Human A431 tumor xenografts were established by subcutaneous inoculation of the mice in the right flank with 1×10^6 A431 cells suspended in 100 μL PBS pH 7.4.[68,69] Tumors were measured using a digital caliper. The tumor volume V (in mm^3) was calculated using the formula $V = (\pi/6)LS^2$ where L is the largest and S is the smallest superficial diameter.

For the pharmacokinetics (PK) study of PTX loaded in mPEG-*b*-p(HPMAm-Bz) micelles, three groups of mice (8 mice per group) were injected with 100 μL of the PTX-loaded micelles (3.2 mg/mL PTX and 27 mg/mL polymer) *via* the tail vein. Blood samples (~80 μL) were collected in tubes with EDTA-anticoagulant *via* submandibular cheek puncture from mice at 0.03, 0.5, 1, 4, 8, and 24 h, respectively, post injection. The plasma was separated from the cell fraction by centrifugation at 1500 g for 10 min, and then 1 vol of plasma was mixed with 2 vol of ACN and vortexed for 1 min followed by centrifugation at 12 000*g* for 5 min. The PTX concentration in the supernatant was measured by UPLC analysis as described above. Control formulations of Taxol and PTX-loaded thermosensitive mPEG-*b*-p(HPMAm-Bz$_{30}$/Nt$_{25}$-*co*-HPMAm-Lac$_{70/75}$) polymeric micelles prepared according to a previously reported method[37] were injected at the same PTX dose (8 mice per group) and blood samples were taken at 0.03 and 24 h after injections.

The biodistribution of PTX was studied by analyzing the PTX concentrations in different organs by UPLC at 24 h after administration of all formulations. The animals were sacrificed (without perfusion with saline) and organs were removed and treated as follows. To 100 mg of organ tissue was added 250 μL of PBS pH 7.4 and the mixture was homogenized by a Bertin tissue grinder at speed of 6000/s for 60 s. The homogenized mixture was mixed with 500 μL of ACN and vortexed for 1 min. The mixture was then centrifuged at 12 000g and the supernatant was collected. The PTX concentration in the supernatant was analyzed by UPLC as described above.

Therapeutic Efficacy Study of PTX-Loaded mPEG-*b*-p(HPMAm-Bz) Micelles in Human A431 and MDA-MB-468 Tumor Xenograft Models. A431 cell culture conditions, mouse strain (female Crl:NU-*Fox^{nu}*1nu mice (22.5 $\pm$ 2.5 g)), housing conditions and inducement of the subcutaneous tumor are described above. When the tumors reached a volume of ~100 mm^3, mice were included in the study. The mice received 100–200 μL iv injections in the tail vein 2 times per week for a total of 10 injections. Each injected dose corresponded with 15 mg/kg PTX in Taxol, and 15 or 30 mg/kg PTX in mPEG-*b*-p(HPMAm-Bz) micelles (equivalent to 120 or 240 mg/kg polymer). Control groups were injected with 200 μL of empty mPEG-*b*-p(HPMAm-Bz) micelles (240 mg/kg polymer) and PBS pH 7.4 with the same dose regimen as the PTX formulations.

MDA-MB-468 cell culture conditions, mouse strain (female Crl:NU-*Fox^{nu}*1nu mice (22.5 $\pm$ 2.5 g)) and housing conditions are described above. MDA-MB-468 tumor xenograft were established by subcutaneous inoculation of the mice in the right flank with 1×10^7 MBA-MD-468 cells suspended in 100 μL cold PBS pH 7.4. When the tumors reached a volume of 80–100 mm^3, mice were included in the study. The mice received 100–200 μL iv injections in the tail vein 1 time per week for a total of 9 injections. Each injected dose corresponded to 15 mg/kg PTX in Taxol, and 15 or 30 mg/kg PTX in mPEG-*b*-p(HPMAm-Bz) micelles (equivalent to 120 or 240 mg/kg polymer). Control groups were injected with 200 μL of empty mPEG-*b*-p(HPMAm-Bz) micelles (240 mg/kg polymer) and PBS pH 7.4 with the same dose regimen as the PTX formulations.

Statistical analyses were performed using GraphPad Prism 5.00 (GraphPad Software, Inc., La Jolla, CA, USA). Differences in tumor growth were analyzed using one-way ANOVA with Bonferroni post-test and survival times were analyzed using the log rank test.

Conflict of Interest: The authors declare no competing financial interest.

Acknowledgment. This research was supported by China Scholarship Council, the European Research Council (ERC Starting Grant 309495: NeoNaNo) and the German Research Foundation (DFG: LA 2937/1-2). C. Rijcken (Crystal Therapeutics BV, Maastricht, The Netherlands) is kindly acknowledged for providing extraction and analytical methods for the detection of paclitaxel in plasma and tissue samples. F. Gremse (Department of Experimental Molecular Imaging (ExMI), Helmholtz Institute for Biomedical Engineering, RWTH Aachen University Clinic, Aachen, Germany) is kindly acknowledged for the technical assistance with the μCT-FMT analysis.

Supporting Information Available: ^{1}H NMR spectra and GPC chromatograms of the (Cy7-labeled) polymer, preparation and characterizations of the Cy7-labeled polymeric micelles loaded with Cy5.5, PTX retention in the mPEG-*b*-p(HPMAm-Bz) micelles, schematic depiction of the workflow employed in the μCT-FMT-based biodistribution analysis, plasma concentrations of PTX after iv injection of the thermosensitive mPEG-*b*-p(HPMAm-Bz$_{30}$/Nt$_{25}$-*co*-HPMAm-Lac$_{70/75}$) micelles in A431 tumor-bearing mice and histopathological analysis of organs of mice treated with different formulations are described. This material is available free of charge *via* the Internet at http://pubs.acs.org.

REFERENCES AND NOTES

1. Kim, S. C.; Kim, D. W.; Shim, Y. H.; Bang, J. S.; Oh, H. S.; Kim, S. W.; Seo, M. H. *In Vivo* Evaluation of Polymeric Micellar Paclitaxel Formulation: Toxicity and Efficacy. *J. Controlled Release* **2001**, *72*, 191–202.
2. Schulz, A.; Jaksch, S.; Schubel, R.; Wegener, E.; Di, Z.; Han, Y.; Meister, A.; Kressler, J.; Kabanov, A. V.; Luxenhofer, R.; et al. Drug-Induced Morphology Switch in Drug Delivery Systems Based on Poly(2-oxazoline)s. *ACS Nano* **2014**, *8*, 2686–2696.
3. Wang, X.; Li, J.; Wang, Y.; Cho, K. J.; Kim, G.; Gjyrezi, A.; Koenig, L.; Giannakakou, P.; Shin, H. J. C.; Tighiouart, M.; et al. HFT-T, a Targeting Nanoparticle, Enhances Specific Delivery of Paclitaxel to Folate Receptor-Positive Tumors. *ACS Nano* **2009**, *3*, 3165–3174.
4. Zhang, R.; Yang, J.; Sima, M.; Zhou, Y.; Kopeček, J. Sequential Combination Therapy of Ovarian Cancer with Degradable *N*-(2-Hydroxypropyl)methacrylamide Copolymer Paclitaxel and Gemcitabine Conjugates. *Proc. Natl. Acad. Sci. U.S.A.* **2014**, *111*, 12181–12186.
5. Nance, E.; Zhang, C.; Shih, T.-Y.; Xu, Q.; Schuster, B. S.; Hanes, J. Brain-Penetrating Nanoparticles Improve Paclitaxel Efficacy in Malignant Glioma Following Local Administration. *ACS Nano* **2014**, *8*, 10655–10664.
6. Zhang, R.; Luo, K.; Yang, J.; Sima, M.; Sun, Y.; Janát-Amsbury, M. M.; Kopeček, J. Synthesis and Evaluation of A Backbone

Biodegradable Multiblock HPMA Copolymer Nanocarrier for the Systemic Delivery of Paclitaxel. *J. Controlled Release* **2013**, *166*, 66–74.
7. Mikhail, A. S.; Allen, C. Poly(ethylene glycol)-*b*-poly(ε-caprolactone) Micelles Containing Chemically Conjugated and Physically Entrapped Docetaxel: Synthesis, Characterization, and the Influence of the Drug on Micelle Morphology. *Biomacromolecules* **2010**, *11*, 1273–1280.
8. Gu, Y.; Zhong, Y.; Meng, F.; Cheng, R.; Deng, C.; Zhong, Z. Acetal-Linked Paclitaxel Prodrug Micellar Nanoparticles as a Versatile and Potent Platform for Cancer Therapy. *Biomacromolecules* **2013**, *14*, 2772–2780.
9. Sun, T.-M.; Du, J.-Z.; Yao, Y.-D.; Mao, C.-Q.; Dou, S.; Huang, S.-Y.; Zhang, P.-Z.; Leong, K. W.; Song, E.-W.; Wang, J. Simultaneous Delivery of siRNA and Paclitaxel *via* a "Two-in-One" Micelleplex Promotes Synergistic Tumor Suppression. *ACS Nano* **2011**, *5*, 1483–1494.
10. Cho, H.; Lai, T. C.; Kwon, G. S. Poly(ethylene glycol)-block-poly(ε-caprolactone) Micelles for Combination Drug Delivery: Evaluation of Paclitaxel, Cyclopamine and Gossypol in Intraperitoneal Xenograft Models of Ovarian Cancer. *J. Controlled Release* **2013**, *166*, 1–9.
11. Cho, H.; Kwon, G. S. Polymeric Micelles for Neoadjuvant Cancer Therapy and Tumor-Primed Optical Imaging. *ACS Nano* **2011**, *5*, 8721–8729.
12. Torchilin, V. P. Micellar Nanocarriers: Pharmaceutical Perspectives. *Pharm. Res.* **2007**, *24*, 1–16.
13. Oerlemans, C.; Bult, W.; Bos, M.; Storm, G.; Nijsen, J. F.; Hennink, W. Polymeric Micelles in Anticancer Therapy: Targeting, Imaging and Triggered Release. *Pharm. Res.* **2010**, *27*, 2569–2589.
14. Deng, C.; Jiang, Y.; Cheng, R.; Meng, F.; Zhong, Z. Biodegradable Polymeric Micelles for Targeted and Controlled Anticancer Drug Delivery: Promises, Progress and Prospects. *Nano Today* **2012**, *7*, 467–480.
15. Kataoka, K.; Harada, A.; Nagasaki, Y. Block Copolymer Micelles for Drug Delivery: Design, Characterization and Biological Significance. *Adv. Drug Delivery Rev.* **2001**, *47*, 113–131.
16. Duan, X.; Xiao, J.; Yin, Q.; Zhang, Z.; Yu, H.; Mao, S.; Li, Y. Smart pH-Sensitive and Temporal-Controlled Polymeric Micelles for Effective Combination Therapy of Doxorubicin and Disulfiram. *ACS Nano* **2013**, *7*, 5858–5869.
17. Cabral, H.; Kataoka, K. Progress of Drug-loaded Polymeric Micelles into Clinical Studies. *J. Controlled Release* **2014**, *190*, 465–476.
18. Matsumura, Y.; Kataoka, K. Preclinical and Clinical Studies of Anticancer Agent-incorporating Polymer Micelles. *Cancer Sci.* **2009**, *100*, 572–579.
19. Eetezadi, S.; Ekdawi, S. N.; Allen, C. The Challenges Facing Block Copolymer Micelles for Cancer Therapy: *In Vivo* Barriers and Clinical Translation. *Adv. Drug Delivery Rev.* **2014**in press.
20. Kim, T.-Y.; Kim, D.-W.; Chung, J.-Y.; Shin, S. G.; Kim, S.-C.; Heo, D. S.; Kim, N. K.; Bang, Y.-J. Phase I and Pharmacokinetic Study of Genexol-PM, a Cremophor-free, Polymeric Micelle-formulated Paclitaxel, in Patients with Advanced Malignancies. *Clin. Cancer Res.* **2004**, *10*, 3708–3716.
21. Lee, K.; Chung, H.; Im, S.; Park, Y.; Kim, C.; Kim, S.-B.; Rha, S.; Lee, M.; Ro, J. Multicenter Phase II Trial of Genexol-PM, a Cremophor-free, Polymeric Micelle Formulation of Paclitaxel, in Patients with Metastatic Breast Cancer. *Breast Cancer Res. Treat.* **2008**, *108*, 241–250.
22. Kim, D.-W.; Kim, S.-Y.; Kim, H.-K.; Kim, S.-W.; Shin, S. W.; Kim, J. S.; Park, K.; Lee, M. Y.; Heo, D. S. Multicenter Phase II Trial of Genexol-PM, a Novel Cremophor-free, Polymeric Micelle Formulation of Paclitaxel, with Cisplatin in Patients with Advanced Non-Small-Cell Lung Cancer. *Ann. Oncol.* **2007**, *18*, 2009–2014.
23. Letchford, K.; Burt, H. M. Copolymer Micelles and Nanospheres with Different *in Vitro* Stability Demonstrate Similar Paclitaxel Pharmacokinetics. *Mol. Pharmaceutics* **2012**, *9*, 248–260.
24. Miller, T.; Breyer, S.; van Colen, G.; Mier, W.; Haberkorn, U.; Geissler, S.; Voss, S.; Weigandt, M.; Goepferich, A. Premature Drug Release of Polymeric Micelles and Its Effects on Tumor Targeting. *Int. J. Pharm.* **2013**, *445*, 117–124.
25. Gaucher, G.; Asahina, K.; Wang, J.; Leroux, J.-C. Effect of Poly(N-vinyl-pyrrolidone)-block-poly(d,l-lactide) as Coating Agent on the Opsonization, Phagocytosis, and Pharmacokinetics of Biodegradable Nanoparticles. *Biomacromolecules* **2009**, *10*, 408–416.
26. Letchford, K.; Liggins, R.; Wasan, K. M.; Burt, H. *In Vitro* Human Plasma Distribution of Nanoparticulate Paclitaxel Is Dependent on the Physicochemical Properties of Poly(ethylene glycol)-block-poly(caprolactone) Nanoparticles. *Eur. J. Pharm. Biopharm.* **2009**, *71*, 196–206.
27. Kim, S.; Shi, Y.; Kim, J. Y.; Park, K.; Cheng, J.-X. Overcoming the Barriers in Micellar Drug Delivery: Loading Efficiency, *in Vivo* Stability, and Micelle–Cell Interaction. *Expert Opin. Drug Delivery* **2010**, *7*, 49–62.
28. Owen, S. C.; Chan, D. P. Y.; Shoichet, M. S. Polymeric Micelle Stability. *Nano Today* **2012**, *7*, 53–65.
29. Chen, H.; Kim, S.; He, W.; Wang, H.; Low, P. S.; Park, K.; Cheng, J.-X. Fast Release of Lipophilic Agents from Circulating PEG-PDLLA Micelles Revealed by *in Vivo* Förster Resonance Energy Transfer Imaging. *Langmuir* **2008**, *24*, 5213–5217.
30. Torchilin, V. Tumor Delivery of Macromolecular Drugs Based on The EPR Effect. *Adv. Drug Delivery Rev.* **2011**, *63*, 131–135.
31. Maeda, H.; Nakamura, H.; Fang, J. The EPR Effect for Macromolecular Drug Delivery to Solid Tumors: Improvement of Tumor Uptake, Lowering of Systemic Toxicity, and Distinct Tumor Imaging *in Vivo*. *Adv. Drug Delivery Rev.* **2013**, *65*, 71–79.
32. van Nostrum, C. F. Covalently Cross-linked Amphiphilic Block Copolymer Micelles. *Soft Matter* **2011**, *7*, 3246–3259.
33. Kwon, G.; Suwa, S.; Yokoyama, M.; Okano, T.; Sakurai, Y.; Kataoka, K. Enhanced Tumor Accumulation and Prolonged Circulation Times of Micelle-forming Poly(ethylene oxide-aspartate) Block Copolymer-adriamycin Conjugates. *J. Controlled Release* **1994**, *29*, 17–23.
34. Talelli, M.; Rijcken, C. J. F.; Hennink, W. E.; Lammers, T. Polymeric Micelles for Cancer Therapy: 3 C's to Enhance Efficacy. *Curr. Opin. Solid State Mater. Sci.* **2012**, *16*, 302–309.
35. Talelli, M.; Iman, M.; Varkouhi, A. K.; Rijcken, C. J.; Schiffelers, R. M.; Etrych, T.; Ulbrich, K.; van Nostrum, C. F.; Lammers, T.; Storm, G.; et al. Core-crosslinked Polymeric Micelles with Controlled Release of Covalently Entrapped Doxorubicin. *Biomaterials* **2010**, *31*, 7797–7804.
36. Yokoyama, M.; Miyauchi, M.; Yamada, N.; Okano, T.; Sakurai, Y.; Kataoka, K.; Inoue, S. Characterization and Anticancer Activity of the Micelle-forming Polymeric Anticancer Drug Adriamycin-Conjugated Poly(ethylene glycol)-poly(aspartic acid) Block Copolymer. *Cancer Res.* **1990**, *50*, 1693–1700.
37. Shi, Y.; van Steenbergen, M. J.; Teunissen, E. A.; Novo, L. S.; Gradmann, S.; Baldus, M.; van Nostrum, C. F.; Hennink, W. E. Π–Π Stacking Increases the Stability and Loading Capacity of Thermosensitive Polymeric Micelles for Chemotherapeutic Drugs. *Biomacromolecules* **2013**, *14*, 1826–1837.
38. Rijcken, C. J.; Snel, C. J.; Schiffelers, R. M.; van Nostrum, C. F.; Hennink, W. E. Hydrolysable Core-crosslinked Thermosensitive Polymeric Micelles: Synthesis, Characterisation and *in Vivo* Studies. *Biomaterials* **2007**, *28*, 5581–5593.
39. Soga, O.; van Nostrum, C. F.; Ramzi, A.; Visser, T.; Soulimani, F.; Frederik, P. M.; Bomans, P. H.; Hennink, W. E. Physicochemical Characterization of Degradable Thermosensitive Polymeric Micelles. *Langmuir* **2004**, *20*, 9388–9395.
40. Shi, Y.; van den Dungen, E. T.; Klumperman, B.; van Nostrum, C. F.; Hennink, W. E. Reversible Addition-fragmentation Chain Transfer Synthesis of a Micelle-forming, Structure Reversible Thermosensitive Diblock Copolymer Based on the *N*-(2-Hydroxy propyl) Methacrylamide Backbone. *ACS Macro Lett.* **2013**, *2*, 403–408.
41. Shi, Y.; Elkhabaz, A.; Yengej, Y.; Fjodor, A.; van den Dikkenberg, J.; Hennink, W. E.; van Nostrum, C. F. Π–Π Stacking Induced

Enhanced Molecular Solubilization, Singlet Oxygen Production, and Retention of a Photosensitizer Loaded in Thermosensitive Polymeric Micelles. *Adv. Healthcare Mater.* **2014**, *3*, 2023–2031.
42. Gong, J.; Chen, M.; Zheng, Y.; Wang, S.; Wang, Y. Polymeric Micelles Drug Delivery System in Oncology. *J. Controlled Release* **2012**, *159*, 312–323.
43. Hamaguchi, T.; Matsumura, Y.; Suzuki, M.; Shimizu, K.; Goda, R.; Nakamura, I.; Nakatomi, I.; Yokoyama, M.; Kataoka, K.; Kakizoe, T. NK105, a Paclitaxel-incorporating Micellar Nanoparticle Formulation, can Extend *in Vivo* Antitumour Activity and Reduce the Neurotoxicity of Paclitaxel. *Br. J. Cancer* **2005**, *92*, 1240–1246.
44. Kunjachan, S.; Gremse, F.; Theek, B.; Koczera, P.; Pola, R.; Pechar, M.; Etrych, T.; Ulbrich, K.; Storm, G.; Kiessling, F.; et al. Nonivsive Optical Imaging of Nanomedicine Biodistribution. *ACS Nano* **2012**, *7*, 252–262.
45. Kunjachan, S.; Pola, R.; Gremse, F.; Theek, B.; Ehling, J.; Moeckel, D.; Hermanns-Sachweh, B.; Pechar, M.; Ulbrich, K.; Hennink, W.; et al. E. Passive *versus* Active Tumor Targeting Using RGD-and NGR-Modified Polymeric Nanomedicines. *Nano Lett.* **2014**, *14*, 972–981.
46. Romberg, B.; Oussoren, C.; Snel, C. J.; Carstens, M. G.; Hennink, W. E.; Storm, G. Pharmacokinetics of Poly-(hydroxyethyl-l-asparagine)-Coated Liposomes Is Superior over that of PEG-Coated Liposomes at Low Lipid Dose and upon Repeated Administration. *Biochim. Biophys. Acta, Biomembr.* **2007**, *1768*, 737–743.
47. Alexis, F.; Pridgen, E.; Molnar, L. K.; Farokhzad, O. C. Factors Affecting the Clearance and Biodistribution of Polymeric Nanoparticles. *Mol. Pharmaceutics* **2008**, *5*, 505–515.
48. Nasongkla, N.; Chen, B.; Macaraeg, N.; Fox, M. E.; Fréchet, J. M.; Szoka, F. C. Dependence of Pharmacokinetics and Biodistribution on Polymer Architecture: Effect of Cyclic *Versus* Linear Polymers. *J. Am. Chem. Soc.* **2009**, *131*, 3842–3843.
49. Etrych, T.; Šubr, V.; Strohalm, J.; Šírová, M.; Říhová, B.; Ulbrich, K. HPMA Copolymer-doxorubicin Conjugates: the Effects of Molecular Weight and Architecture on Biodistribution and *in Vivo* Activity. *J. Controlled Release* **2012**, *164*, 346–354.
50. Theek, B.; Gremse, F.; Kunjachan, S.; Fokong, S.; Pola, R.; Pechar, M.; Deckers, R.; Storm, G.; Ehling, J.; Kiessling, F.; et al. Characterizing EPR-mediated Passive Drug Targeting Using Contrast-enhanced Functional Ultrasound Imaging. *J. Controlled Release* **2014**, *182*, 83–9.
51. Bertrand, N.; Leroux, J.-C. The journey of a Drug-carrier in the Body: An Anatomo-Physiological Perspective. *J. Controlled Release* **2012**, *161*, 152–163.
52. Kamaly, N.; Xiao, Z.; Valencia, P. M.; Radovic-Moreno, A. F.; Farokhzad, O. C. Targeted Polymeric Therapeutic Nanoparticles: Design, Development and Clinical Translation. *Chem. Soc. Rev.* **2012**, *41*, 2971–3010.
53. Kwon, I. K.; Lee, S. C.; Han, B.; Park, K. Analysis on the Current Status of Targeted Drug Delivery to Tumors. *J. Controlled Release* **2012**, *164*, 108–114.
54. Fetterly, G.; Straubinger, R. Pharmacokinetics of Paclitaxel-Containing Liposomes in Rats. *AAPS PharmSci.* **2003**, *5*, 90–100.
55. Yang, T.; Cui, F.-D.; Choi, M.-K.; Cho, J.-W.; Chung, S.-J.; Shim, C.-K.; Kim, D.-D. Enhanced Solubility and Stability of PE-Gylated Liposomal Paclitaxel: *in Vitro* and *in Vivo* Evaluation. *Int. J. Pharm.* **2007**, *338*, 317–326.
56. Kim, S. C.; Kim, D. W.; Shim, Y. H.; Bang, J. S.; Oh, H. S.; Kim, S. W.; Seo, M. H. *In Vivo* Evaluation of Polymeric Micellar Paclitaxel Formulation: Toxicity and Efficacy. *J. Controlled Release* **2001**, *72*, 191–202.
57. Rijcken, C. J. Tuneable & Degradable Polymeric Micelles for Drug Delivery: from Synthesis to Feasibility *in Vivo*. Doctoral dissertation; Utrecht University, Utrecht, 2007.
58. Aliabadi, H. M.; Lavasanifar, A. Polymeric Micelles for Drug Delivery. *Expert Opin. Drug Delivery* **2006**, *3*, 139–62.
59. Liu, L.; Li, C.; Li, X.; Yuan, Z.; An, Y.; He, B. Biodegradable Polylactide/poly(ethylene glycol)/polylactide Triblock Copolymer Micelles as Anticancer Drug Carriers. *J. Appl. Polym. Sci.* **2001**, *80*, 1976–1982.
60. Jeong, Y. I.; Cheon, J. B.; Kim, S. H.; Nah, J. W.; Lee, Y. M.; Sung, Y. K.; Akaike, T.; Cho, C. S. Clonazepam Release from Core-Shell Type Nanoparticles *In Vitro*. *J. Controlled Release* **1998**, *51*, 169–78.
61. Song, B.; Wang, Z.; Chen, S.; Zhang, X.; Fu, Y.; Smet, M.; Dehaen, W. The Introduction of $\Pi-\Pi$ Stacking Moieties for Fabricating Stable Micellar Structure: Formation and Dynamics of Disklike Micelles. *Angew. Chem., Int. Ed.* **2005**, *117*, 4809–4813.
62. Dosio, F.; Brusa, P.; Crosasso, P.; Arpicco, S.; Cattel, L. Preparation, Characterization and Properties *in Vitro* and *in Vivo* of a Paclitaxel-Albumin Conjugate. *J. Controlled Release* **1997**, *47*, 293–304.
63. Katragadda, U.; Fan, W.; Wang, Y.; Teng, Q.; Tan, C. Combined Delivery of Paclitaxel and Tanespimycin *via* Micellar Nanocarriers: Pharmacokinetics, Efficacy and Metabolomic Analysis. *PLoS One* **2013**, *8*, e58619.
64. Li, C.; Newman, R. A.; Wu, Q.-P.; Ke, S.; Chen, W.; Hutto, T.; Kan, Z.; Brannan, M. D.; Charnsangavej, C.; Wallace, S. Biodistribution of Paclitaxel and Poly(L-glutamic acid)-Paclitaxel Conjugate in Mice with Ovarian OCA-1 Tumor. *Cancer Chemother. Pharmacol.* **2000**, *46*, 416–422.
65. Le Garrec, D.; Gori, S.; Luo, L.; Lessard, D.; Smith, D.; Yessine, M.-A.; Ranger, M.; Leroux, J.-C. Poly(*N*-vinylpyrrolidone)-block-poly(d,l-lactide) as a New Polymeric Solubilizer for Hydrophobic Anticancer Drugs: *In Vitro* and *in Vivo* Evaluation. *J. Controlled Release* **2004**, *99*, 83–101.
66. Neradovic, D.; Van Nostrum, C.; Hennink, W. Thermoresponsive Polymeric Micelles with Controlled Instability Based on Hydrolytically Sensitive *N*-Isopropylacrylamide Copolymers. *Macromolecules* **2001**, *34*, 7589–7591.
67. Shi, Y.; Kunjachan, S.; Wu, Z.; Gremse, F.; Moeckel, D.; Zandvoort, M. v.; Kiessling, F.; Storm, G.; Nostrum, C. F. v.; Hennink, W. E.; et al. Fluorophore-Labeling of Core-Crosslinked Polymeric Micelles for Multimodal *in Vivo* and *ex Vivo* Optical Imaging. *Nanomedicine (London)* **2015**, in press, DOI: 10.2217/nnm.14.170.
68. Safavy, A.; Bonner, J. A.; Waksal, H. W.; Buchsbaum, D. J.; Gillespie, G. Y.; Khazaeli, M.; Arani, R.; Chen, D.-T.; Carpenter, M.; Raisch, K. P. Synthesis and Biological Evaluation of Paclitaxel-C225 Conjugate as a Model for Targeted Drug Delivery. *Bioconjugate Chem.* **2003**, *14*, 302–310.
69. Zhang, Y.; Xiang, L.; Hassan, R.; Paik, C. H.; Carrasquillo, J. A.; Jang, B.-S.; Le, N.; Ho, M.; Pastan, I. Synergistic Antitumor Activity of Taxol and Immunotoxin SS1P in Tumor-Bearing Mice. *Clin. Cancer Res.* **2006**, *12*, 4695–4701.